RSC Advances

ROYAL SOCIETY OF CHEMISTRY

www.rsc.org/advances

RSC Advances

RSCPublishing

ARTICLE

Influences of sodium dodecyl sulfate on vulcanization kinetics and mechanical performance of EPDM/graphene oxide nanocomposites†

Cite this: DOI: 10.1039/x0xx00000x

Received 00th January 2012,
Accepted 00th January 2012

DOI: 10.1039/x0xx00000x

www.rsc.org/

Ahmad Allahbakhsh[a]* and Saeedeh Mazinani[b]

In this study, the influences of sodium dodecyl sulfate (SDS) on vulcanization process and mechanical performance of ethylene-propylene-diene-monomer rubber (EPDM)/graphene oxide (GO) nanocomposites are investigated. Torque values variations and activation energies of the vulcanization process are used to study possible interactions between GO and EPDM. An increase in physical interactions between EPDM macromolecules and GO nanosheets in the presence of SDS is observed through rheometry studies, as minimum torque and scorch time of the vulcanization process increased noticeably. Moreover, the maximum strength of EPDM/GO nanocomposite in the presence of SDS is about 137% more than mechanical strength of EPDM/GO nanocomposite. Furthermore, EPDM/GO nanocomposite is elongated up to 700% in the presence of SDS. A mechanism for physical interactions between EPDM macromolecules and GO nanosheets and influences of SDS presence on such interactions is reported based on Fourier transform infrared spectroscopies.

1. Introduction

Recently, graphene as a two-dimensional carbon-based nanomaterial has attracted superior attention for many novel potential applications in different industries. This wide range of possible applications originates from outstanding properties of graphene such as high mechanical, electrical and optical properties.[1-3] Most of the known potential applications of graphene are reported in its polymer nanocomposite forms.[4, 5] This is why most of the recent studies in the polymer arena are focused on presenting and modifying novel and efficient methods for the preparation of graphene-based polymer nanocomposites.

One of the most interested engineering polymers is ethylene-propylene-diene rubber (EPDM) which has been used in applications such as automotive sealing, the sidewalls of tires, cover stripes, wires, cables and industrial hoses.[6-8] EPDM as an unsaturated polyolefin rubber has magnificent resistance to ozone and oxidation, low-temperature flexibility and color stability.[9] Therefore, EPDM/graphene nanocomposites are expected to have a high potential for applications from space to automotive industries.[10-12] However, due to the tendency of graphene to agglomerate in combination with large species such as polymeric macromolecules, surface modification of graphene seems essential to achieve a reasonable dispersion degree of graphene.

The oxidation of graphene is widely reported as a routine method for the reaching exfoliated morphology in graphene-based polymer nanocomposites.[10, 13, 14] Almost all recent studies on graphene reinforced polymer nanocomposites have reported enhanced graphene dispersion in its oxidized form.[15-17] Moreover, graphene oxide (GO) can easily disperse in solvents to form an approximately stable GO suspension. However, further surface modifications of GO may lead to advanced improvements on the GO dispersion in a polymer matrix.[18]

Sodium dodecylbenzenesulfonate (SDBS) and its relative sodium dodecyl sulfate (SDS) are two known graphite-based nanomaterials surfactants, which have been widely used for the preparation of stable suspension of GO nanosheets and carbon nanotubes. However, recent studies suggest that molecular interactions between polymer macromolecules and GO nanosheets decrease in the presence of hyper molecules of SDBS on GO surface.[19] SDS is a cationic linear surfactant which has been widely used for the complete dispersion of graphene in polymeric nanocomposites.[20-22] The SDS presence noticeably affects wettability and interfacial adhesion of graphene-like fillers in polymer matrixes.[23]

Unlike SDBS, molecules of SDS are more linear and there are no benzene groups in the structure of SDS. Such a structure results in more flexibility, which can increase potential reinforce-ability of graphene through more interactions with

polymer macromolecules. However, nature of the polymer matrix and the final nanocomposite chemical state are two important factors that should be considered for the selection of the most appropriate graphene modifier, besides dispersing agent structure.

In this work, the influences of SDS as a GO dispersing agent on the vulcanization process and mechanical performance of EPDM/GO nanocomposites are studied. It has been reported that GO nanosheets affect the vulcanization process of elastomers through interactions with accelerator systems.[10, 24] Moreover, it is expected that GO nanosheets affect the density of chemical crosslinks formed during the vulcanization process.[10] In this study, the effects of SDS on the activation energy, vulcanization process and crosslink density of EPDM/GO nanocomposites are reported and compared to the non-modified compound. In previous works, vulcanization kinetics parameters of fast curing (cure process at 180 and 190 °C) were also included in activation energy calculations.[10] In this study, however, cure process is just limited to low-temperature vulcanization processes, which is relatively longer and less affected by temperature. In addition, the influences of SDS on structural behavior and mechanical performance of vulcanized nanocomposites are also reported.

2. Experimental

2.1. Materials

Graphite powder used in this study was from LECO Company and SDS powder was found from Merck Chemicals Company. EPDM (grade Vistalon 7500; Mooney Viscosity ML 1 + 8 at 125°C, ethylene content 56 %, ethylidene norbornene (ENB) content 5.7 %) was from ExxonMobil Corporation. All used solvents were provided from Merck Chemicals Company. Moreover, rubber curing additives were commercial-grade and used as received.

2.2. Preparation of GO and GO-SDS powders

GO was prepared through oxidation of graphite powder using a modified technique based on Hummers' method reported in the literature.[25, 26] In a typical procedure, 1 g of graphite powder was put into a round bottom flask and 100 ml of sulfuric acid (98%) was added into the flask. Afterward, the mixture was stirred and gradually, 6 g of potassium permanganate ($KMnO_4$) was added to the mixture. The mixture was allowed to react for 4 h at 75-80 °C and 300 ml of distilled water was added to the reaction mixture. After 15 min, the reaction was terminated by adding 50 ml of H_2O_2 (25 ml, 30%) aqueous solution resulting in a yellow-brown solution. Finally, the mixture was washed with HCl solution (10%) and water until the neutral pH of the filtrate was reached.

In order to prepare GO suspension, graphite oxide was sonicated for 20 min. To remove the un-exfoliated graphite oxide particles, the mixture was centrifuged for 10 min to obtain the graphene oxide suspension. The GO suspension was gradually sprayed out on the glass surface kept at 110 °C and then was separated layer by layer from the surface to achieve the multi-layered graphene oxide powder. To prepare GO-SDS suspension, 0.5 weight % SDS was added to the GO suspension (1 g GO / 100 ml water) and the mixture was sonicated. The prepared GO-SDS suspension was powdered according to the procedure described above for GO powdering at 110 °C.

2.3. Preparation of nanocomposites

EPDM, GO powder, GO-SDS powder and other ingredients such as zinc oxide (ZnO), strearic acid, N-cyclohexyl-2-benzothiazolesulfenamide (CBS) and sulfur were compounded using a Rodolfo Comerio laboratory-sized two-roll mill (350 mm × 700 mm) at ambient temperature for about 15 min. The compounds were vulcanized in a 150 bar Dr. Collin GmbH Laboratory mold for optimum curing times (t_{90}) at 170 °C. The recipe for preparing nanocomposites through this study is summarized in **Table 1**.

Table 1 Recipes of the compounds (indicated in phr: parts per hundred parts of rubber)

Ingredient	EPDM	EPDM/3phr GO	EPDM/3phr GO-SDS
EPDM	100	100	100
Sulfur	2	2	2
ZnO	5	5	5
Stearic acid	1.5	1.5	1.5
CBS*	1	1	1
GO	--	3	--
GO-SDS	--	--	3

*N-Cyclohexyl-2-Benzothiazolesulfenamide

2.4. Characterization and measurements

Atomic force microscopy (AFM) images of prepared GO and GO-SDS was obtained using a Dualscope DS 95-200, DME atomic force microscope. Samples for AFM were developed on a freshly cleaved mica surface. Chemical characteristics of GO-SDS nanosheets as well as nanocomposites were characterized using a Nicolet IR100 Fourier transform infrared (FTIR) spectrometer. Field emission scanning electron microscopy (FESEM) images of prepared nanocomposites were provided employing a Hittachi S4160 scanning electron microscope. X-ray diffraction (XRD) patterns were presented using a Inel Equinox 3000 diffractometer (Cu k_α radiation (λ= 1.54056 Å) at 40 kV and 30 mA).

Tensile tests of dumbbell-shaped specimens prepared of vulcanized samples were carried out on a Hiwa 200 universal testing machine at a speed of 500 mm/min according to ASTM D412. True (Cauchy) stress and true (Hencky) strain results were calculated from 3 repeats of tensile tests according to the literature.[27] Moreover, true stress values at the quasi-linear region (approximately at 50% elongation) were used in the calculation of elastic modulus values. The cure characteristics of the compounds were obtained by means of torque curves using a Hiwa 900 moving die rheometer (MDR) according to ASTM D5289 at 150, 160 and 170 °C.

Transmission electron microscopy (TEM) images of prepared nanocomposites were provided using a Zeiss EM10C TEM at an accelerating voltage of 80 kV. Ultra-thin sections for TEM images were prepared using a Reichert OMU3 ultramicrotome equipped with a diamond knife.

2.5. Model for describing the cure kinetics

Vulcanization behavior of rubber compounds can be studied through evaluation of rheometric data (minimum and maximum time-depended torque values) as well as model-derived cure characteristics (reaction activation energy, rate constant and reaction order). The degree of curing process (ϑ) can be calculated from the time-depended torque values through the following equation:[10]

$$\vartheta = (M_t - M_{min}) / (M_{max} - M_{min}) \quad (1)$$

where M_t, M_{min} and M_{max} are torque values at a given time of cure process, the minimum torque (also shown with ML) and the maximum torque (also shown with MH) values, respectively.

A number of empirical models are available for modeling the vulcanization of elastomeric materials.[28] One of the most common models for describing the kinetics of the cure process in elastomeric materials is the model presented by Isayev and Deng.[29] Isayev-Deng model is reported as the best model for describing cure process in EPDM/GO systems as the most reliable vulcanization characteristics can be obtained using this model.[10] In this model, the state of cure (θ) for isothermal vulcanization process is expressed as follows:[10]

$$\vartheta = k (t - t_s)^n / 1 + k (t - t_s)^n \quad (2)$$

where t and t_s are the time of reaction and scorch time, respectively and k is the rate constant for the vulcanization process. Scorch time is defined as the test time at which the torque rise from the minimum point (M_L) initiates.[30] Moreover, k in the nth order reactions represents temperature-dependent reaction rate constant defined via well known Arrhenius equation as:

$$k = k_0 \exp(-E / RT) \quad (3)$$

where k_0, E, R and T are factors of reaction velocity, activation energy, gas constant and absolute temperature, respectively. Moreover, k_0 represents the incidence of molecular collisions that should be obtained for a chemical reaction to occur.

In this work, computational fitting was used for the calculation of Isayev-Deng model constants. In a typical calculation, the conversion versus time curve obtained using equation 1 was fitted to equation 2. In this way, cure reaction order (n) and rate constant (k) values were calculated through fitting process for three different cure temperatures (160, 170 and 180 °C). The activation energy was calculated via equation 3 using k and T values as input. The fitting computations were done using MATLAB software version 7.12.0.635. Parameters were measured through data fitting on models with more than 90 % goodness of fit.

2.6. Crosslink density measurements

The crosslink density amounts of prepared compounds were measured according to the solvent-swelling theory via applying Flory–Rehner equation on volume changes of compounds immersed in toluene (99%) for 72 h at 25 °C. Flory–Rehner equation is presented in equation 4:[10]

$$M_c = (-\rho V_s V_r^{1/3}) / (\ln(1-V_r) + V_r + \chi V_r^2) \quad (4)$$

where M_c, ρ and V_s are the mean molecular weight between two adjacent crosslinks, the density of EPDM (0.9 g/cm^3) and molar volume of solvent (107.0 mL/mol for toluene), respectively. V_r is the volume fraction of the swollen rubber and χ is the interaction coefficient between the rubber network and solvent (0.038), which V_r and χ can be calculated using equations 5 and 6, respectively:[10]

$$V_r = 1 / (1 + Q_m) \quad (5)$$

$$\chi = (\delta_s - \delta_r) V_s / RT \quad (6)$$

where Q_m, δ_s and δ_r are the swelling weights of the compounds in toluene and the solubility parameters of solvent and rubber network, respectively (8.9 for toluene and 8 for EPDM). Moreover, R and T in equation 6 are the universal gas constant (8.314 J/mol K) and the absolute temperature, respectively. The degree of crosslink density (n) can be measured using equation 7, which is the sum of physical and chemical crosslinks.

$$n = 1 / (2M_c) \quad (7)$$

3. Results and discussion

3.1. Characterization of GO-SDS nanosheets

AFM technique was used for the characterization of GO-SDS nanosheets thickness distribution as shown in **Figure 1**. Two tapping-mode AFM images of GO-SDS nanosheets in bulk and corresponding height distribution curves were shown in Figure 1 (a) and (b). The thickness values of nanosheets as presented AFM images in Figure 1 (a) and (b) were 2.3 and 1.5 nm, respectively. Moreover, the overall height distribution diagram of GO-SDS nanosheets in bulk was also presented in Figure 1 (c). The distribution diagram depicted a narrow height distribution and majority of GO-SDS nanosheets had a thickness of about 2 nm in bulk. The thickness of an individual GO nanosheet is reported about 1.5 nm in the literature and as a result, most of the prepared GO-SDS nanosheets in this work were single or few-layers nanosheets.[18]

FTIR method was employed to characterize chemical structure of prepared GO-SDS nanosheets as shown in **Figure 2**. FTIR spectrum of GO-SDS nanosheets comprised three bands at wavenumbers around 430, 460 and 590 cm^{-1} assigned to C–H deformation vibrations.[18] The band at 879 cm^{-1} originated from

asymmetrical stretching vibration of C–O–S bonds.[31] The observed band at 1056 cm^{-1} originated from symmetrical stretching vibration of S=O bonds. Moreover, The characteristic band of C–O–C bond of GO epoxide groups (see peak at 1007 cm^{-1} in FTIR spectrum of GO presented in Figure S1) was observed on the right shoulder of band at 1056 cm^{-1}. Furthermore, the absorption band at 1195 cm^{-1} has been reported as the characteristic band of S–O stretching vibrations of SO_4 groups.[31, 32]

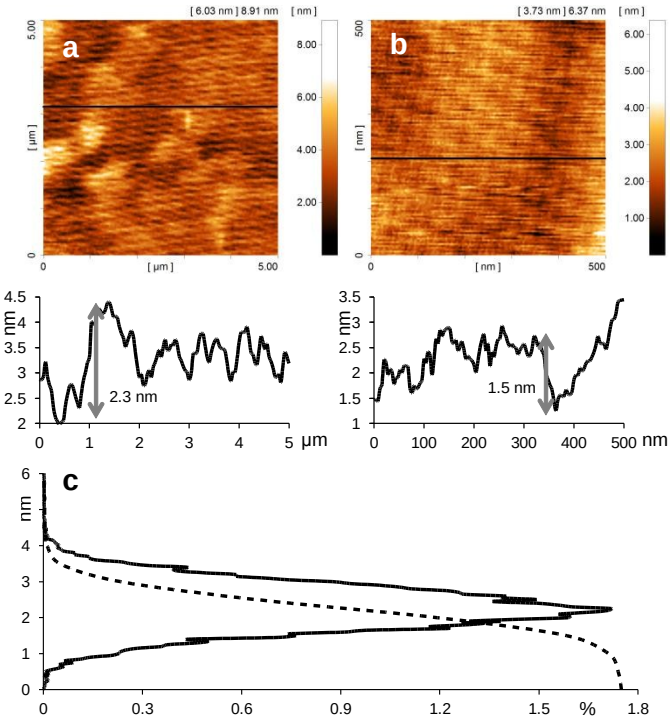

Figure 1 AFM images and corresponding image height curves (a and b) as well as overall height distribution diagram of GO-SDS nanosheets (c)

The band at 1419 cm^{-1} was corresponding to asymmetrical bending of C–H bonds in the structure of SDS. Moreover, the band observed at around 1520 cm^{-1} originated from C=C bond stretching vibrations of GO skeleton.[18] Furthermore, two observed bands at wavenumbers around 1643 and 1704 cm^{-1} were related to the vibrational mode of the ketone (–C=O) groups.[33] The band appeared at 2360 cm^{-1} contributed to –OH stretching vibration.[13] The asymmetric and symmetric stretching of $–CH_2–$ groups in the structure of SDS were assigned to the strong bands at 2923 and 2854 cm^{-1}, respectively.[31] In addition, bands at 3417, 3748 and 3856 cm^{-1} originated from the stretching vibrations of residual water molecules.

Recently, we proposed an interaction mechanism between GO nanosheets and SDBS cationic molecules, which suggested non-covalent interactions between GO nanosheets and $–SO_4$ group in SDBS molecules.[19] However, recent studies proved that GO surface is strongly charged negatively and the negative charge of GO surface increase with the content of oxygen-containing groups.[34, 35] As a result, it can be concluded that SDS adsorbs on GO nanosheets surface due to hydrophobic interactions. However, electrostatic repulsion between GO nanosheets and negatively charged SDS prevents adsorption of SDS on GO surface.

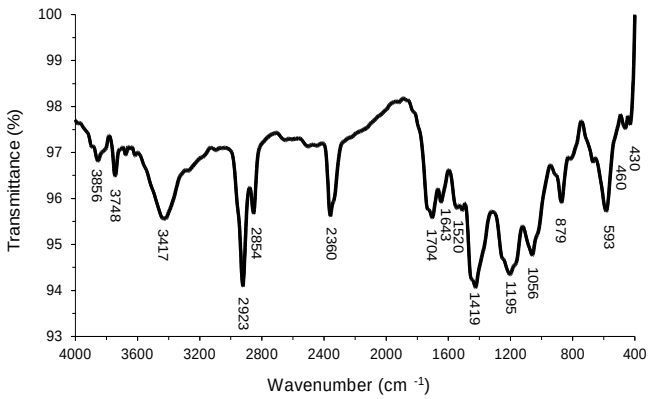

Figure 2 FTIR spectrum of GO-SDS nanosheets

Molecular structure of SDS, a reported structural model for GO nanosheets (Gao et al. model[36]) and a proposed interaction mechanism between SDS and GO nanosheets are depicted in **Figure 3**. SDS molecules consist of a sulfate hydrophilic molecular part ($–SO_4$) and a hydrocarbon hydrophobic segment. The interaction between GO nanosheets surface and the hydrophilic sulfate group of SDS is suggested to be the source of mentioned electrostatic repulsion forces, as GO surface and sulfate groups are both negatively charged.[31, 37] Thus, the interactions between alkane groups of SDS and GO nanosheets surface should be the adsorption mechanism of SDS on GO and as a result, the characteristic peak of bending vibration of $–CH_3$ (band at 1350 cm^{-1} in Figure S1) should not be seen in FTIR spectrum of GO-SDS nanosheets.

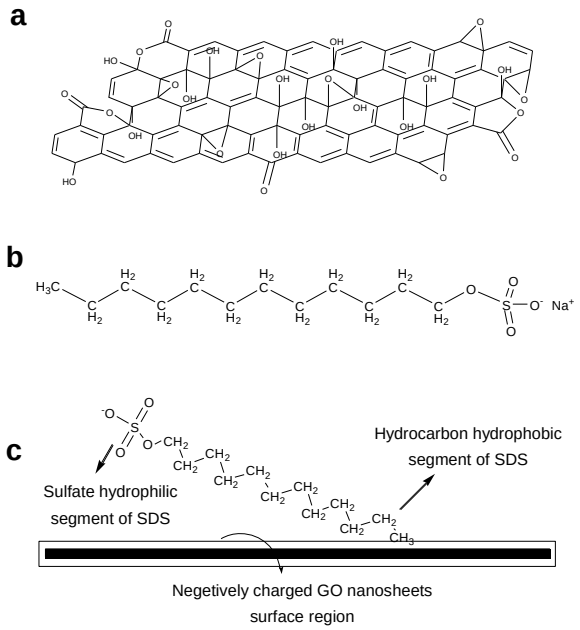

Figure 3 Structural model proposed by Gao et al. for GO nanosheets (a), molecular structure of SDS (b) and interaction mechanism of SDS and GO nanosheets surface (c)

3.2. Structural and morphological studies

XRD patterns of GO-SDS nanosheets as well as EPDM/3phr GO-SDS nanocomposite were used to investigate the influences of SDS on structural performance of nanocomposites, as shown in **Figure 4**. The XRD pattern of GO-SDS nanosheets contained a single weak peak at 2θ around 29°. There is no sign of strong peaks at 2θ values around 20 and 22° in Figure 4, which is an evidence for the absence of segregated crystalline SDS particles.[38] Moreover, there is no sign of graphite and GO reflection peaks at 2θ values around 26 and 10°, respectively. This reveals that GO nanosheets were in an appropriate range of dispersion in the presence of SDS as a surfactant.

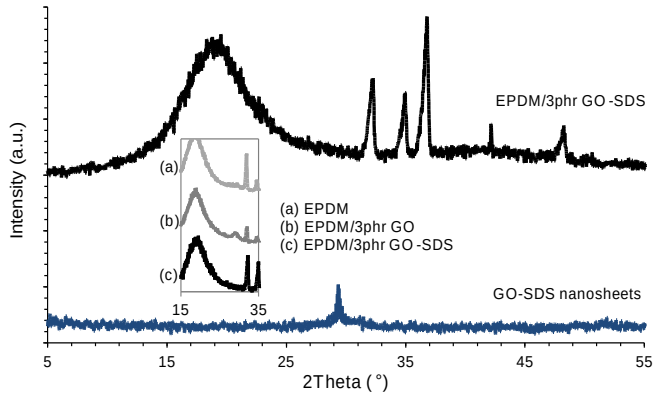

Figure 4 XRD patterns of GO-SDS nanosheets and EPDM/3phr GO-SDS nanocomposite

XRD pattern of EPDM/3phr GO-SDS nanocomposite involved a broad peak for amorphous rubber structures with a center at 2θ around 18°. Moreover, three characteristic peaks of hexagonal wurtzite structure of zinc oxide (ZnO) were observed at 32, 35 and 36°.[10] Noticeably, there is no sign of peak at 2θ values around 29° in the XRD pattern of EPDM/3phr GO-SDS nanocomposite, observed in XRD results of GO-SDS nanosheets and 3phr GO loaded nanocomposite. One possible explanation for such a behavior is that the observed peak relates to the structure of crumpled GO nanosheets formed during powdering process.[26] In the presence of SDS, GO nanosheets dispersed more uniformly in the polymer matrix during milling process and as a result, no sign of GO nanosheets peak at 2θ values around 10° nor graphite characteristic peak at 2θ values around 26° were observed in Figure 4.

Morphological performance of EPDM/3phr GO-SDS nanocomposite is compared with the morphology of 3phr GO loaded nanocomposite using TEM and FESEM images presented in **Figure 5**. Generally, no significant difference between GO and GO-SDS loaded nanocomposites were observed regarding nanosheets distribution in Figure 5. However, observed smaller nanoparticles in Figures 5 (a) and (b), compared to the mean particle size of nanoparticles in Figures 5 (c) and (d), express the idea that a higher degree of nanosheets dispersion was achieved in the presence of SDS as a surfactant. This is in close accordance with the discussed structural performance of EPDM/3phr GO-SDS nanocomposite in discussions regarding Figure 4.

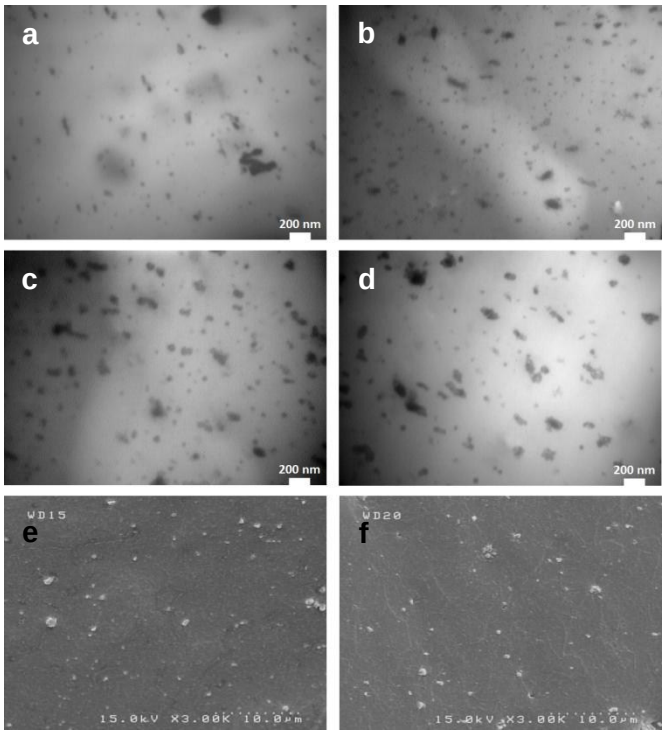

Figure 5 TEM images (a and b) and FESEM image (e) of EPDM/3phr GO-SDS nanocomposite as well as TEM images (c and d) and FESEM image (f) of EPDM/3phr GO nanocomposite

Generally, high shear tension during direct compounding of EPDM and GO nanosheets through milling process results in a high degree of size reduction in GO nanosheets and formation of thin and small GO nanosheets. In the presence of SDS, however, thickness and size of these nanosheets reduced noticeably (comparing Figures 5 (b) and (d) for instance). Moreover, the size and number of 200-400 nm GO aggregates in Figures 5 (a) and (b) are smaller than observed aggregates in Figures (c) and (d). Therefore, presence of SDS resulted in formation of less GO aggregates through powdering process and perhaps, more exfoliation of GO aggregates during milling process. By comparing TEM and FESEM images, it can be concluded that the observed white nanoparticles in Figure 5 are probably these discussed crumpled GO nanosheets. In the presence of SDS as a GO surfactant, however, the mean size of these nanoparticles in Figure 5 (f) reduced noticeably and simultaneously, the broad peak at 2θ values around 29° disappeared in Figure 4. Moreover, the observed white particles in micron dimensions through Figure 5 (e) and (f) were accelerator particles, as used ZnO and CBS for vulcanization of EPDM in this work were of commercial grade.[10]

3.3. Mechanical properties studies

Stress-strain graphs of tensile tests were used to investigate the influences of SDS presence on mechanical performance of prepared nanocomposites, as shown in **Figure 6**. The low-strain

mechanical performance of prepared nanocomposites, which can be considered as mechanical performance at the quasi-linear region, was significantly different. As depicted in Figure 6, EPDM/3phr GO-SDS nanocomposite presented an enhanced mechanical performance in this region, compared to EPDM and EPDM/3phr GO nanocomposite. However, 3phr GO loaded nanocomposite shown a decrease in mechanical performance in comparison with the unfilled EPDM sample in this region. This variation in mechanical performance of nanocomposites can be related to the dispersion degree of nanosheets in EPDM matrix as well as more structural solidarity of GO-SDS loaded nanocomposite.

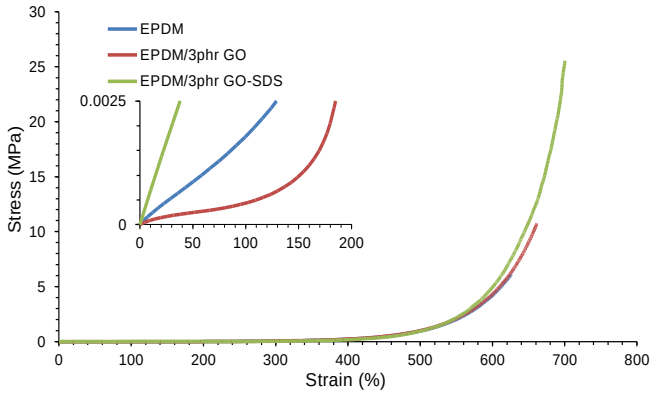

Figure 6 Stress-strain curves of cured EPDM sample as well as EPDM/3phr GO and EPDM/3phr GO-SDS nanocomposites

Mechanical characteristics of samples in Figure 6 are also summarized in **Table 2** for closer investigations. The maximum strength of EPDM/3phr GO-SDS nanocomposite enhanced noticeably to 25.54 MPa, which is about 137% higher than maximum strength of EPDM/3phr GO nanocomposite. Moreover, maximum strength of 3phr GO-SDS loaded nanocomposite increased about 318%, compared to non-reinforced EPDM sample. Such an enhancement in mechanical performance was not achieved even in the presence of considerably higher contents of graphene nanoplatelets and carbon black in the structure of EPDM.[11]

Table 2 Mechanical characteristics of prepared compounds

Compounds	Elongation at break (%)	Maximum strength (MPa)	Strength at 100% elong. (kPa)	Elastic modulus (Pa)
EPDM	626	6.11	1.63	18.55
EPDM/3phr GO	662	10.75	0.13	7.14
EPDM/3phr GO-SDS	700	25.54	6.29	66.89

We believe that such a high level of enhancement in mechanical strength of EPDM, with very low GO-SDS nanosheets loading (3phr) and without using any carbon black additive in the compounding recipe, is due to strong structural connectivity of EPDM/3phr GO-SDS nanocomposite due to the high degree of chemical crosslinks as well as physical interactions. GO nanosheets in a dispersed form can reinforce rubber materials through interactions of GO nanosheets surface with rubber macromolecules. Such interactions are not expected in the case of non-functionalized graphene-reinforced nanocomposites.

The values of elongation at break for prepared compounds are also reported in Table 2. Elongation at break can be considered as a benchmark for the rubber-like behaviour of elastomeric materials. EPDM/3phr GO-SDS nanocomposite was elongated up to 700% before breakage in tensile test, which is about 40% more than 3phr GO loaded nanocomposite. Elongation extent of rubber compounds can represent the contents of crosslinks formed during the vulcanization process. Such a mechanical performance is a clear proof for the formation of more crosslinks between EPDM macromolecules in the presence of GO-SDS nanosheets, compared to the unfilled and GO loaded systems.

3.4. Vulcanization kinetics studies

Cure kinetics' studies were carried out using Isayev-Deng model, presented in equation 2, as the conversion-time pattern for calculation of cure kinetics' data (k and n), which in turns used for activation energy measurements. The torque vs. time curves, the cure reaction conversion vs. normalized cure reaction time (t-t_s) curves and the theoretical fitting curves obtained using Isayev-Deng model are presented in **Figure 7**. Due to very low filler loadings (3phr), the fully dominated interaction mechanism in this study is filler-polymer interactions.[39] Generally, SDS presence resulted in a decrease in maximum and minimum torque differences for completion of cure process (see Figure S2 for torque-time curves of EPDM and EPDM/3phr GO samples).

To investigate cure behavior of prepared samples in details, cure characteristics of prepared compounds are summarized in **Table 3**. Minimum and maximum torque values represent a qualitative overview of rubber macromolecules dynamics during the vulcanization process. Minimum torque values were in a close range for all samples. Maximum torque values, however, varied noticeably for unfilled and filled compounds. Vulcanization of compounds at low temperatures (150 °C) comparably can more clearly monitor influences of nanosheets interactions than vulcanization at higher temperatures. Cure process at low temperatures is long (about an hour) and heat can, consequently, transfer throughout the sample more homogenously. Therefore, torque values at low temperatures are more affected by interactions between EPDM and GO than by applied temperatures. At moderate and high temperatures (170 °C), however, cure process is comparably shorter (about half of an hour) and as a result, torque values are more affected by influences of nanosheets presence on thermal conductivity on one hand and, on the other hand, diffusion of accelerator systems.

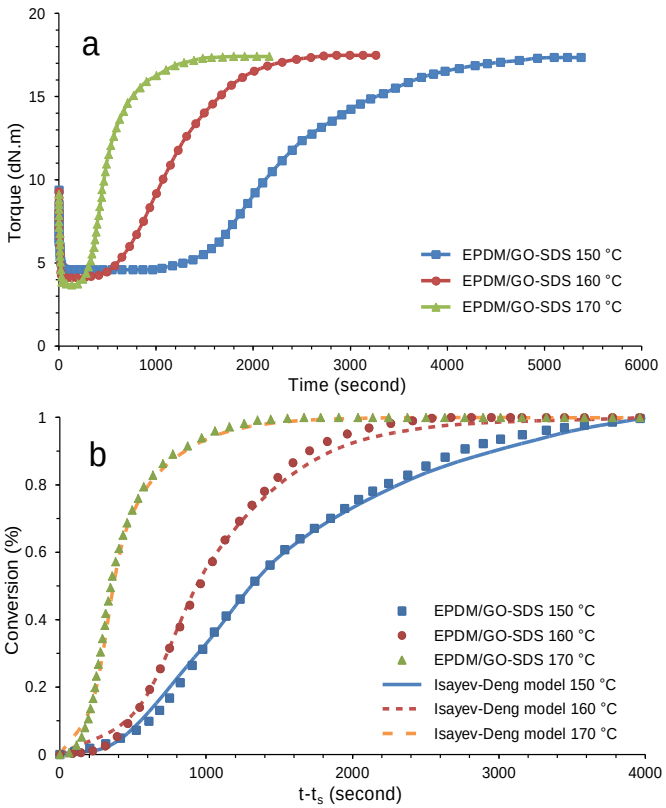

Figure 7 Torque-time (a) and vulcanization conversion-time (b) curves of EPDM/3phr GO-SDS nanocomposite at three vulcanization temperatures (lines in Figure 7 (b) represent fitting results of conversion-time data in Eq. 2)

Minimum torque values of GO and GO-SDS loaded nanocomposites were higher than non-reinforced EPDM. Minimum torque value, which is the torque required to maintain a specified rotation amplitude at a constant frequency at opening stages of the vulcanization process, can be used to monitor physical interactions between polymer and nanosheets. Increase in ML values in the presence of GO and GO-SDS nanosheets is because of physical interactions between polymer and GO nanosheets, which results in fewer movements of polymer macromolecules. However, it should be noted that only ML values at low cure temperatures (150 and 160 °C) can be used to investigate physical interactions, as at high temperatures (170 °C) high thermal conductivity of GO nanosheets results in more heat transfer and more flexibility of macromolecules and as a result, less ML values for nanocomposites.

Scroch time values of GO and GO-SDS nanosheets loaded nanocomposites also increased noticeably, compared to EPDM. This value demonstrates required time for overcoming interactions between GO nanosheets and EPDM macromolecules, before formation of any chemical crosslinks. In addition, cure of GO and GO-SDS nanosheets loaded samples completed through very slower processes, compared to EPDM. Longer cure process of compounds can be assumed as a sign of more chemical-crosslinks formation between polymer macromolecules.

Table 3 Cure characteristics of prepared compounds

Compounds	Cure temperature (°C)	ML (dN.m)	MH (dN.m)	t_s (min)	t_{10} (min)	t_{50} (min)	t_{90} (min)	t_{cure} (min)
EPDM	150	4.28	19.15	4.28	12.5	21	33	47.16
	160	3.86	27.95	0.88	9.98	14.89	25.68	44.12
	170	3.72	28.46	1.44	4.49	7.24	14.13	23.98
EPDM/3phr GO	150	4.36	15.55	11	21.04	30.95	46.08	57.63
	160	3.91	22.79	4.41	11.01	20.35	44.37	67.03
	170	3.51	22.96	1.84	4.49	8.34	21.42	48.14
EPDM/3phr GO-SDS	150	4.59	17.35	16.06	26.18	38.26	62.19	87.24
	160	4.12	17.48	3.05	10.78	19.08	31.48	47.61
	170	3.67	17.41	2.17	5.39	7.94	15.03	29.96

By considering maximum torque value of samples at final steps of the vulcanization process, we can find a clearer insight regarding cure completion steps. Maximum torque value can be assumed as a sign of elastic behavior of vulcanized compounds. More MH values mean less elongation and flexibility of vulcanization process products. By considering MH value traces for prepared compounds at different temperatures, it can be seen that EPDM/3phr GO nanocomposite shown more flexibility to the rotation than non-reinforced EPDM sample (lower MH values in comparison with the non-reinforced EPDM). Moreover, vulcanized EPDM/3phr GO-SDS nanocomposite required fewer MH values (more flexibility to rotation) in comparison with GO loaded nanocomposite, as well as non-reinforced EPDM sample. These results are in close accordance with observed elongation behavior of cured compounds. Therefore, cure process of EPDM/GO nanocomposite in the presence of SDS resulted in a clear increase not only in mechanical strength (maximum strength), but also in maximum elongation (elongation at break and MH) of final compound.

Vulcanization kinetics' parameters of prepared compounds measured using Isavey-Deng model are summarized in **Table 4**. Cure process of prepared compounds was an *n*th order chemical reaction with reaction orders in the range of 2.4-2.6. Required activation energy values as well as reaction rate constant values were used to investigate the influences of SDS presence on vulcanization kinetics of EPDM/GO nanocomposites. Heat transfer throughout the sample and movability of macromolecules can affect activation energy values, as reported in the literature.[10]

Table 4 Vulcanization kinetics parameters of Isayev-Deng model

Compounds	Cure temperature (°C)	k (s^{-1})	n	E_a (kJ/mol)
EPDM	150	1.532×10^{-8}	2.621	213.21
	160	1.834×10^{-8}	2.635	
	170	2.406×10^{-7}	2.600	
EPDM/3phr GO	150	2.515×10^{-8}	2.497	240.37
	160	6.719×10^{-8}	2.405	
	170	5.543×10^{-7}	2.400	
EPDM/3phr GO-SDS	150	2.077×10^{-8}	2.469	229.77
	160	1.793×10^{-8}	2.610	
	170	4.062×10^{-7}	2.500	

Activation energy value increased in the case of EPDM/3phr GO nanocomposite, compared to non-reinforced EPDM. Reported results in this work are based on the vulcanization process of EPDM compounds at only low temperatures, due to the purposes of physical interaction studies. Therefore, there is a conflict between reported results in this work and our earlier publication.[10] However, we believe reported results in this work measured through the cure process at only low temperatures can monitor cure characteristics of compounds more precisely. Our reason for such a claim is that cure process at low temperatures is less affected by temperature and more depended on curing ingredients.

Higher values of activation energy for GO and GO-SDS loaded nanocomposites, compared to EPDM, are due to more chemical crosslinks between polymer macromolecules in the presence of GO nanosheets. Moreover, GO loaded nanocomposite shown higher activation energy value than EPDM/3phr GO-SDS nanocomposite. This can be due to more chemical-crosslinks formed between polymer macromolecules during vulcanization of EPDM/3phr GO nanocomposite. Therefore, it can be concluded that EPDM/3phr GO nanocomposite had more chemical crosslinks than GO-SDS loaded nanocomposite, which in turns had more chemical crosslinks than non-reinforced EPDM sample.

Moreover, activation energy of the vulcanization process can be considered as the energy required to overcome internal interactions between polymer macromolecules to participate in the vulcanization process. Therefore, this parameter can be seen as a symbol of physical interactions between polymer and GO nanosheets, which limit molecular movability of polymer macromolecules. As a result, it can be concluded that there are more physical interactions between GO and EPDM macromolecules than between GO-SDS and EPDM macromolecules. This conclusion needs more investigation of physical and chemical interactions in the structure of prepared compounds, which will be discussed in cure studies.

3.5. Vulcanization process and chemical studies

Vulcanization process of EPDM using CBS as the accelerator has been studied thoroughly in the literature.[10] The emphasis here is on the influences of SDS presence on possible interactions between EPDM macromolecules and GO nanosheets during sulfur-based cure process using CBS as an accelerator. In this regard, one of the main reasons for the elimination of carbon black from the compounding recipe in this study was to investigate the possible interactions between EPDM and GO nanosheets in a system without any extra additives. FTIR spectrum of EPDM/3phr GO-SDS, shown in **Figure 8**, was used to study the chemical structure of vulcanized nanocomposite.

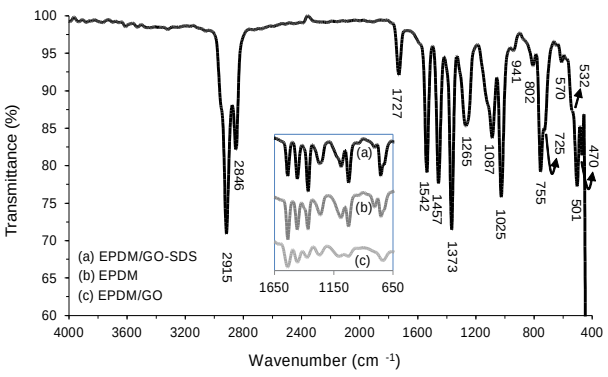

Figure 8 FTIR spectrum of EPDM/3phr GO-SDS nanocomposite

FTIR spectrum of EPDM/3phr GO-SDS nanocomposite contained three bands at 470, 501 and 532 cm^{-1} corresponding to C–H deformation vibrations.[10] Moreover, band appeared at 570 cm^{-1} was related to C–S stretching.[40] Bands appeared at 725, 755 and 802 cm^{-1} originated from deformation vibrations of $(–CH_2)_n$ groups ($n \geq 5$) in the ethylene portions of the EPDM backbone.[41] Band appeared at 941 cm^{-1} represents C=C groups of ENB sequences in the structure of EPDM.[41] In addition, bands at wavenumbers around 1025, 1087 and 1265 cm^{-1} represent C–O–C bonds in the structure of residual accelerator derviatives.[42]

Bands at wavenumbers around 1373 and 1457 cm^{-1} were assigned to the vibrations of the $–CH_3$ and $–CH_2$ groups of propylene segments of EPDM backbone, respectively.[41] Moreover, bands appeared at wavenumbers around 1542 and 1727 cm^{-1} originated from *endo*-cyclic C=C bond of ENB groups and C=O bond of functional groups formed during oxidation process, respectively.[43] Furthermore, bands at wavenumbers around 2846 and 2915 cm^{-1} were related to the asymmetric and symmetric stretching modes of C–H bonds in aliphatic CH_2 groups.

Molecular structure of EPDM and suggested molecular reorientations between ENB groups of two EPDM macromolecules during the vulcanization process are presented in **Figure 9**. Reaction of CBS molecules with zinc oxide and stearic acid results in formation of activated polysulfide precursors, which in turns can be converted to sulfur-based crosslinks between polymer macromolecules, as reported in the literature.[10] Moreover, it was suggested that sulfur vulcanization of EPDM macromolecules from 9-position in ENB groups labeled in Figure 9 is always preferred over 3-exo position which in turns, is always preferred over the 3-endo position.[44, 45] Therefore, it can be suggested that EPDM vulcanization consists of reaction between polysulfide precursor with a 9-position carbon in ENB group of one macromolecule, followed by reaction of jointed precursor with a 9-position or 3-exo position carbon in another macromolecule.

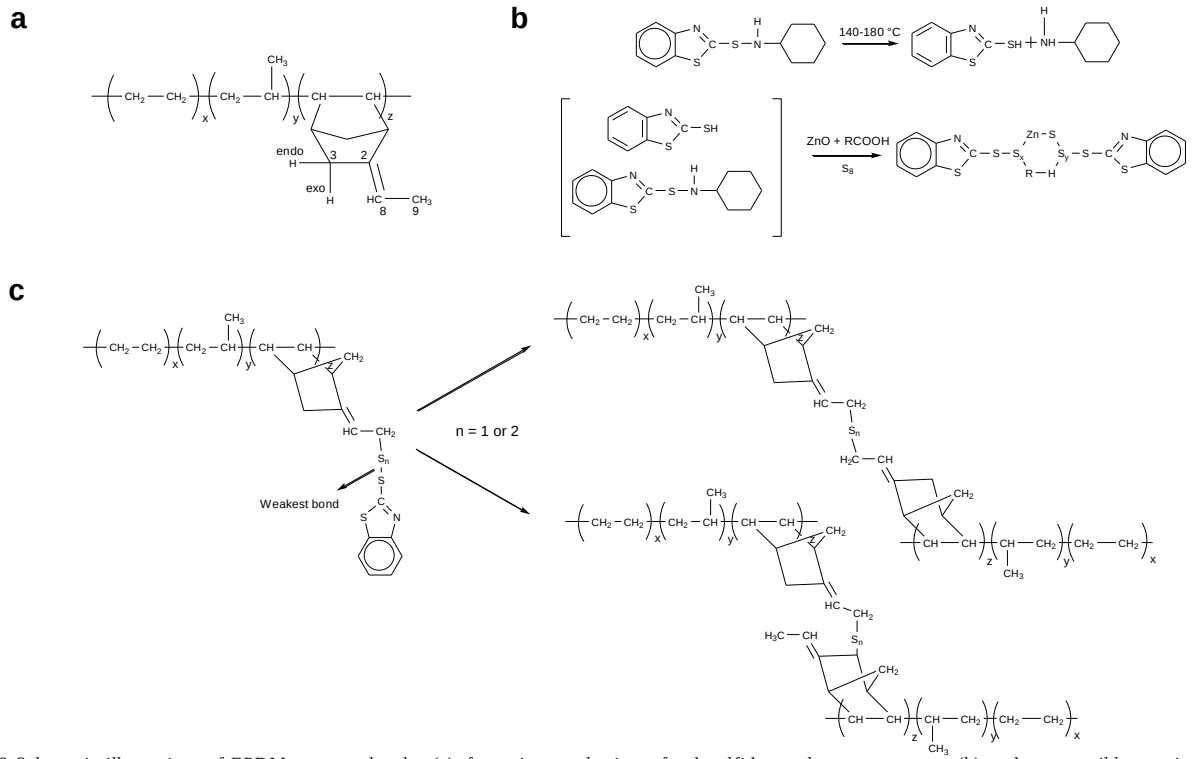

Figure 9 Schematic illustrations of EPDM macromolecules (a), formation mechanism of polysulfide accelerator precursors (b) and two possible reactions for sulfur-based vulcanization of EPDM (c)

It was reported that prolonged vulcanization of EPDM at temperatures higher than 150 °C can result in oxidation and reversion of crosslinked EPDM macromolecules.[44] Oxidation of sulfur-based crosslinks in Figure 9 (c) results in formation of carbonyl groups through oxidation of 9-position and/or 3-exo position carbons. Moreover, it was reported that oxidation process could take place directly through oxidation of ENB groups of EPDM macromolecules.[44] However, oxidation of 9-position and 3-exo position carbons of sulfur crosslinks seems more likely to occur. Three possible products which can be formed during the oxidation process of vulcanized EPDM are shown in Figure 10 (a).

The suggested interaction mechanisms between EPDM macromolecules and graphene nanosheets in two forms of GO and GO-SDS are schematically depicted in **Figure 10**. In the case of EPDM/3phr GO nanocomposite, the intensity (depth) of FTIR bands dedicated to ethylene sequences (750, 802, 2846 and 2915 cm^{-1}) and propylene portions (1350 and 1450 cm^{-1}) reduced noticeably, compared to the corresponding bands in the spectrum of EPDM. This indicates that EPDM macromolecules

interacted with the surface region of GO nanosheets through ethylene and propylene parts of the chain. Such interactions, can result in highly immobilized EPDM macromolecules, which can form physical crosslinks near facial regions of GO nanosheets.[19] Moreover, the intensity of FTIR bands assigned to accelerator systems (1025, 1087 and 1260 cm^{-1}) decreased for 3phr GO loaded nanocomposite, compared to the unfilled EPDM sample. This behavior is a clear proof for the proposed interactions between GO nanosheets and the accelerator system, reported in the literature based on XRD observations.[10]

In the presence of SDS as the GO surfactant, however, a clear change in interaction mechanism between macromolecules and nanosheets was observed. No reduction in intensity of FTIR bands assigned to ethylene and propylene sequences of EPDM chains, nor in the intensity of bands related to the accelerator system was observed. The only observed differences between FTIR spectra of EPDM and EPDM/3phr GO-SDS nanocomposite were in the depth of FTIR bands at 802 and 1542 cm^{-1} related to –C–H bond of long ethylene segments and C=C bonds of ENB groups, respectively.

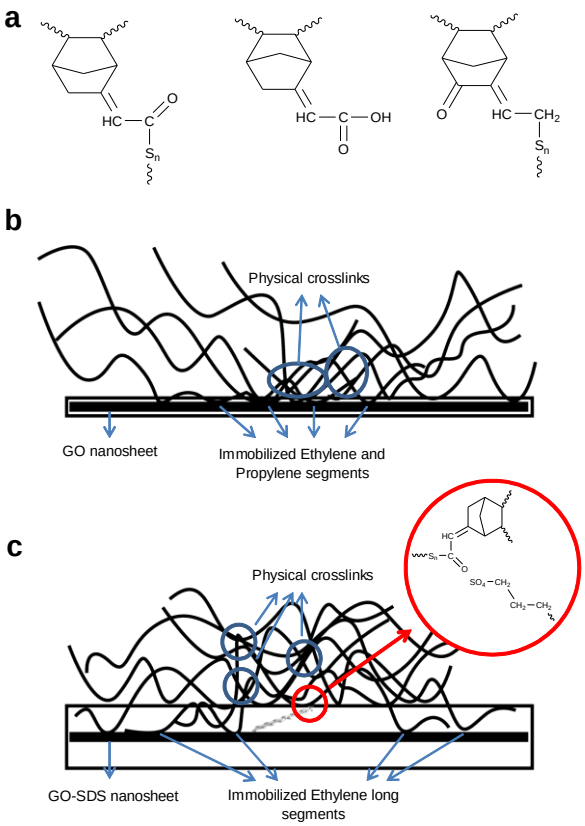

Figure 10 Schematic illustrations of: oxidation mechanisms of vulcanized EPDM macromolecules during cure process (a), suggested interaction mechanism between GO nanosheets and EPDM long chains (b) as well as suggested interaction mechanism between GO-SDS nanosheets and EPDM macromolecules (c)

As depicted in Figure 8, the depth of FTIR band at 1542 cm^{-1} assigned to C=C bonds reduced in the case of EPDM/3phr GO-SDS nanocomposite, compared to the unfilled EPDM sample. In addition, there is no sign of free SO_4 groups of SDS in Figure 8 (peak at 1195 cm^{-1} in Figure 2). Therefore, it can be concluded that interactions between GO-SDS nanosheets and EPDM macromolecules include some surface interactions between ethylene long segments of EPDM and GO surface as well as some more interactions between SO_4 groups of SDS and C=C bonds of ENB groups. The nature of these interactions should be non-covalent, as there is no sign of C–O–S asymmetrical stretching vibration characteristic band in Figure 8 (band at 879 cm^{-1} in Figure 2). These interactions result in more mobility of EPDM chains in the sulfur-based cure process which in turns leads to more chemical crosslinks between EPDM macromolecules. Moreover, immobilized segments near GO surface and SO_4 groups of SDS tend to form local physical crosslinks. Thus, EPDM/3phr GO-SDS nanocomposite is expected to have more chemical crosslinks than EPDM/3phr GO nanocomposite, which in turns results in more structural solidarity due to the high degree of physical and chemical crosslinks.

The densities of crosslinks formed through vulcanization of prepared compounds were measured using Flory–Rehner theory to investigate the influences of 3phr GO and GO-SDS loading on the content of physical and chemical crosslinks of nanocomposites, as shown in **Figure 11**. As discussed, the contents of chemical and physical crosslinks increase in the presence of GO and GO-SDS nanosheets. It can be due to formation of physical crosslinks via immobilized EPDM macromolecules. EPDM/3phr GO nanocomposite comprised some degree of physical crosslinks, compared to EPDM sample. This resulted in about 10 % increase in the contents of formed crosslinks during the vulcanization process of GO loaded nanocomposite in comparison with the unfilled EPDM sample. Moreover, more mobility of EPDM macromolecules in the case of EPDM/3phr GO-SDS nanocomposite resulted in formation of more chemical crosslinks, besides formation of physical crosslinks. As a result, the contents of crosslinks for GO-SDS loaded nanocomposite were about 31 % more than the unfilled sample and about 18 % more than GO loaded nanocomposite.

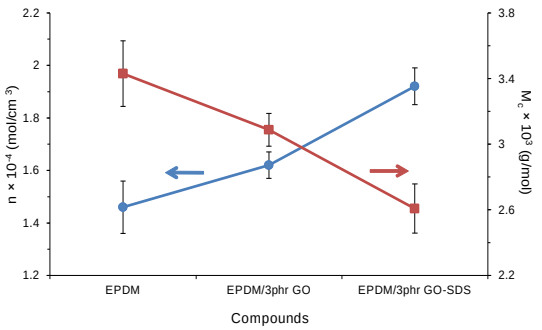

Figure 11 Crosslink density (n) and molecular weight between crosslinks (M_c) variations of EPDM sample as well as EPDM/3phr GO and EPDM/3phr GO-SDS nanocomposites

Conclusions

In this study, influences of SDS, as a GO surfactant, on mechanical and structural properties as well as the vulcanization process of EPDM/GO nanocomposites were studied. Based on XRD results, GO nanosheets were dispersed appropriately through nanocomposites in the presence of SDS. High level of GO dispersion was also confirmed through FESEM images of vulcanized EPDM/GO nanocomposites. In addition, mechanical characteristics of EPDM/GO nanocomposites enhanced considerably in the presence of SDS. Maximum strength and elongation at break of EPDM/GO-SDS nanocomposite increased noticeably in comparison with GO loaded nanocomposite. The strength of GO-SDS loaded nanocomposite increased to values around 25 MPa, which is much higher than maximum strength of nanocomposites filled with larger amounts of graphene nanoplatelets and carbon black. High degree of physical and chemical crosslinks formed during the vulcanization process was reported as the main reason for the observed mechanical performance.

Vulcanization kinetics were studied via rheometry results and activation energy values, calculated using Isayev-Deng model. The assess of minimum torque values revealed a high degree of physical interactions between GO and EPDM macromolecules. Moreover, activation energies of prepared nanocomposites increased in the presence of GO nanosheets. This means that required energy for completion of the vulcanization process increased in the presence of SDS as a surfactant. FTIR method and crosslink density measurements were used to investigate the vulcanization process of EPDM/GO-SDS nanocomposite. Based on FTIR results, a possible mechanism for interactions between EPDM macromolecules and GO-SDS nanosheets was presented. This mechanism involved non-covalent interactions between ENB parts of EPDM chains and SO_4 groups of SDS as well as physical interactions between ethylene segments and the GO surface region.

Acknowledgements

The authors would like to thank "Mahar Fan Abzar Co." for AFM results and Mr. Hossein Ghasempour Ch. for his invaluable help.

Notes and references

[a] Young Researchers and Elite Club, Shiraz Branch, Islamic Azad University, Shiraz, Iran.

*Corresponding Author: ahmad.allahbakhsh@gmail.com , a.allahbakhsh@modares.ac.ir

[b] Amirkabir Nanotechnology Research Institute (ANTRI), Amirkabir University of Technology, Tehran, Iran.

† Electronic Supplementary Information (ESI) available: FTIR spectrum of GO nanosheets, torque-time curves of EPDM and EPDM/3phr GO nanocomposite, reaction rate-degree curves of EPDM/3phr GO-SDS at different vulcanization temperatures and Arrhenius plot of rate constants of Isayev-Deng model. See DOI: 10.1039/b000000x/

1. Y. Chen, Y. Qi, Z. Tai, X. Yan, F. Zhu and Q. Xue, *European Polymer Journal*, 2012, **48**, 1026-1033.
2. F. Scarpa, S. Adhikari and A. Srikantha Phani, *Nanotechnology*, 2009, **20**, 065709.
3. Y. Zhu, S. Murali, W. Cai, X. Li, J. W. Suk, J. R. Potts and R. S. Ruoff, *Advanced Materials*, 2010, **22**, 3906-3924.
4. T. Kuilla, S. Bhadra, D. Yao, N. H. Kim, S. Bose and J. H. Lee, *Progress in Polymer Science*, 2010, **35**, 1350-1375.
5. J. R. Potts, D. R. Dreyer, C. W. Bielawski and R. S. Ruoff, *Polymer*, 2011, **52**, 5-25.
6. A. K. Maity and S. F. Xavier, *European Polymer Journal*, 1999, **35**, 173-181.
7. K. A. J. Dijkhuis, J. W. M. Noordermeer and W. K. Dierkes, *European Polymer Journal*, 2009, **45**, 3302-3312.
8. P. Li, L. Yin, G. Song, J. Sun, L. Wang and H. Wang, *Applied Clay Science*, 2008, **40**, 38-44.
9. A. A. Wazzan, *International Journal of Polymeric Materials*, 2005, **54**, 783-794.
10. A. Allahbakhsh, S. Mazinani, M. R. Kalaee and F. Sharif, *Thermochimica Acta*, 2013, **563**, 22-32.
11. L. Valentini, A. Bolognini, A. Alvino, S. Bittolo Bon, M. Martin-Gallego and M. A. Lopez-Manchado, *Composites Part B: Engineering*, 2014, **60**, 479-484.
12. B. Chen, N. Ma, X. Bai, H. Zhang and Y. Zhang, *RSC Advances*, 2012, **2**, 4683.
13. X. Wang, J. Jin and M. Song, *European Polymer Journal*, 2012, **48**, 1034-1041.
14. A. Allahbakhsh, M. Sheydaei, S. Mazinani and M. Kalaee, *High Performance Polymers*, 2013, **25**, 576-583.
15. H. Kim, Y. Miura and C. W. Macosko, *Chemistry of Materials*, 2010, **22**, 3441-3450.
16. X. Zhao, Q. Zhang, D. Chen and P. Lu, *Macromolecules*, 2010, **43**, 2357-2363.
17. Y. Huang, Y. Qin, Y. Zhou, H. Niu, Z.-Z. Yu and J.-Y. Dong, *Chemistry of Materials*, 2010, **22**, 4096-4102.
18. A. Allahbakhsh, F. Sharif and S. Mazinani, *Nano*, 2013, **08**, 1350045.
19. A. H. Haghighi, M. Sheydaei, A. Allahbakhsh, M. Ghatarband and F. S. Hosseini, *Journal of Thermal Analysis and Calorimetry*, 2014, **117**, 525-535.
20. J. Yang, M. Tian, Q.-X. Jia, J.-H. Shi, L.-Q. Zhang, S.-H. Lim, Z.-Z. Yu and Y.-W. Mai, *Acta Materialia*, 2007, **55**, 6372-6382.
21. H. Hu, X. Wang, J. Wang, L. Wan, F. Liu, H. Zheng, R. Chen and C. Xu, *Chemical Physics Letters*, 2010, **484**, 247-253.
22. E. Tkalya, M. Ghislandi, A. Alekseev, C. Koning and J. Loos, *Journal of Materials Chemistry*, 2010, **20**, 3035.
23. T. Jeevananda, Siddaramaiah, N. H. Kim, S.-B. Heo and J. H. Lee, *Polymers for Advanced Technologies*, 2008, **19**, 1754-1762.
24. J. Wu, W. Xing, G. Huang, H. Li, M. Tang, S. Wu and Y. Liu, *Polymer*, 2013, **54**, 3314-3323.
25. W. S. Hummers and R. E. Offeman, *Journal of the American Chemical Society*, 1958, **80**, 1339-1339.
26. A. Allahbakhsh, F. Sharif, S. Mazinani and M. R. Kalaee, *Int. J.Nano Dimens.*, 2014, **5**, 11-20.
27. S. N. Raman, T. Ngo, J. Lu and P. Mendis, *Materials & Design*, 2013, **50**, 124-129.
28. A. Arrillaga, A. M. Zaldua, R. M. Atxurra and A. S. Farid, *European Polymer Journal*, 2007, **43**, 4783-4799.
29. A. I. Isayev and J. S. Deng, *Rubber Chem. Technol.*, 1988, **61**, 340-361.
30. T. H. Khang and Z. M. Ariff, *Journal of Thermal Analysis and Calorimetry*, 2011, **109**, 1545-1553.
31. L. Zhao and L. Gao, *Journal of Materials Chemistry*, 2004, **14**, 1001.
32. Z. Mo, Y. Sun, H. Chen, P. Zhang, D. Zuo, Y. Liu and H. Li, *Polymer*, 2005, **46**, 12670-12676.
33. D. W. Lee, L. De Los Santos V, J. W. Seo, L. L. Felix, A. Bustamante D, J. M. Cole and C. H. W. Barnes, *The Journal of Physical Chemistry B*, 2010, **114**, 5723-5728.
34. E. Hashemi, O. Akhavan, M. Shamsara, R. Rahighi, A. Esfandiar and A. R. Tayefeh, *RSC Advances*, 2014, **4**, 27213.
35. M. Tang, T. Wu, X. Xu, L. Zhang and F. Wu, *Mater. Res. Bull.*, 2014, **60**, 118-129.
36. W. Gao, L. B. Alemany, L. Ci and P. M. Ajayan, *Nature Chemistry*, 2009, **1**, 403-408.
37. L. Jiang, L. Gao and J. Sun, *J. Colloid Interface Sci.*, 2003, **260**, 89-94.
38. M. H. Huang, B. S. Dunn, H. Soyez and J. I. Zink, *Langmuir*, 1998, **14**, 7331-7333.

39. S. M. Hosseini and M. Razzaghi-Kashani, *Polymer*, 2014, **55**, 6426-6434.
40. K. Sahakaro, A. G. Talma, R. N. Datta and J. W. M. Noordermeer, *J. Appl. Polym. Sci.*, 2007, **103**, 2547-2554.
41. S. Samaržija-Jovanović, V. Jovanović, G. Marković, S. Konstantinović and M. Marinović-Cincović, *Composites Part B: Engineering*, 2011, **42**, 1244-1250.
42. G. C. Basak, A. Bandyopadhyay, S. Neogi and A. K. Bhowmick, *Appl. Surf. Sci.*, 2011, **257**, 2891-2904.
43. I. Y. Shchapin, O. V. Makhnach, V. L. Klochikhin, Y. G. Osokin and A. I. Nekhaev, *Petroleum Chemistry*, 2007, **47**, 92-98.
44. R. Winters, W. Heinen, M. A. L. Verbruggen, J. Lugtenburg, M. van Duin and H. J. M. de Groot, *Macromolecules*, 2002, **35**, 1958-1966.
45. M. A. L. Verbruggen, L. van der Does, J. W. M. Noordermeer and M. van Duin, *J. Appl. Polym. Sci.*, 2008, **109**, 976-986.

